Volume 13, Number 3, 2020. pp. 191-199

Jordan Journal of Physics

ARTICLE

Analysis of the Various Effects of Coating W Tips with Dielectric Epoxylite 478 Resin or UPR-4 Resin Coatings under Similar Operational Conditions

A. Al Soud[a], **A. Knápek**[b] and **M. S. Mousa**[a]

[a] *Surface Physics and Materials Technology Lab, Department of Physics, Mutah University, Al-Karak 61710, Jordan.*

[b] *Institute of Scientific Instruments of the CAS, Královopolská 147, 612 64 Brno, Czech Republic.*

Doi : https://doi.org/10.47011/13.3.2

Received on: 28/11/2019; Accepted on: 10/4/2020

Abstract: The objective of this work is to study the differences that occur in behavior and properties of the emitted electron beam from tungsten (W) tips before and after coating these tips with a thin layer of a good proven dielectric material. Core metallic tips have been prepared from a polycrystalline (99.995% purity) tungsten (W) wire. Analysis has been carried out for clean W emitters before and after coating these tips with two differences types of epoxy resins; namely: (Epoxylite 478 and UPR-4). For critical comparison and analysis, several tungsten tips with various apex- radii (very sharp) have been prepared with the use of electrochemical etching techniques. The tips have been coated by dielectric thin films of various thicknesses. Their characteristics have been recorded before and after the process of coating. These measurements have included the current-voltage (I-V) characteristics, Fowler-Nordheim (F-N) plots, visible light microscope (VLM) image and scanning electron microscope (SEM) micrographs to measure the influence of the Epoxylite resin coating's thickness on the tips after coating. Special distributions have been recorded from the phosphorescent screen of a field electron emission microscope as well. Comparing the two sets of composite systems tested under similar conditions has provided several advantages. Recording highly interesting phenomena has produced a wide opportunity to develop a new type of emitter that includes the most beneficial features of both types.

Keywords: Cold field emission, Epoxylite 478, Epoxylite UPR-4..

Introduction

Field electron emission (FEE) is a process of electron emission from the surface of metals into vacuum due to an intense applied external electric field E > 10^9 V /m [1]. The emitter is usually formed into a tiny tip, which has an apex radius ranging from several nanometers to micrometers. When preparing very sharp field emitters, it is essential to use a metal with the possibly highest quality. In this work, experiments have used polycrystalline Tungsten from high-purity tungsten wires. Due to the favorable properties of those Polycrystalline Tungsten emitters, such as the highest melting point (3650 K) of all the pure metals, the second-highest of all over the periodic table after carbon, high hardness (strength), work function (4.5 eV) and heat resistance at high temperature [2], this type of emitter sources has been widely used in this field research. Within this work, tungsten

Corresponding Author: Marwan S. Mousa **Email**: mmousa@mutah.edu.jo

micrometers with different apex radii ranging from 100-150 nm have been prepared and coated with a thin layer of various types of epoxylite resins (Epoxylite 478 resins or Epoxylite UPR-4 resins), where the thickness of epoxy layer range is 40-70 nm by using electron microscopes to extract the tip's profile and thickness of epoxy layer (i.e., apex radii). The emission images were directly photographed from the phosphor screen of the field electron microscope (FEM), using a digital camera. The current-voltage (I-V) measurements and Fowler–Nordheim (F-N) plots have been carried out under vacuum (UHV) conditions with a base pressure of about 10^{-7} Pa.

Experimental Techniques

The tungsten emitters have been prepared by electrolytic etching. A 0.1mm tungsten wire is immersed into an electrolyte 2 molar (NaOH) solution, where the emitter was placed in a stainless steel conductive cylinder. The anode (emitter) and the cathode (steel cylinder) have been immersed into the (NaOH) solution and connected to a DC power source (12 V). The time taken to etch is around 5 minutes and when immersing approx. (0.6-0.8) cm of tungsten wire into NaOH solution, the etching current started at approx. 4 μA and its value is decreased as the wire becomes thinner with time and continued until the bottom part of the wire is dropped off. There were many requirements needed to be followed to prepare very sharp tips [5]: 1) sufficient surface wettability of the etched wire. 2) sufficient chemical clarity of the used chemicals. 3) accurate depth when immersing the wire. 4) etching source capable of disconnecting the etch current in a very short time. 5) sufficient immunity to mechanical vibrations. Fig. 1 shows the experimental setup to electrical etching and coating. When the bottom part drops off, the resistance of the etching circuit suddenly increases and then, the DC voltage source is quickly switched off. At large, the switch-off time in the etching system greatly affects the sharpness of the tip. Then, the W wire has been carefully pulled from the solution, where the tip was immediately cleaned by carefully dipping it into alcohol and distilled water for a few seconds, respectively. Besides, the tip has been placed in the ultrasonic bath for 15 minutes to clean it from the oxide layers formed on the tip surface [6].

To coat the emitter with a 60-nm thick epoxy layer (using commercial resins marked: Epoxylite 478 resins and Epoxylite UPR-4 resins), the tip has to be immersed 4 times into the resin very slowly and vertically as follows: the sample holder that keeps the sample in a vertical position is mounted on a trolley that moves vertically and lowers into a flask of epoxylite resin and the tip while a 90° angle between the surface of the epoxylite resin and the tip is maintained [7]. To ensure an even distribution of resin on the surface of the tip and stabilize the epoxylite resin on tip surface, the coated tip is transferred into a furnace and subjected to 30-minute curing at 373 K to drive off the solvent, followed by thirty minutes at 453 K to complete the curing of the resin [2,7].

Then, the composite emitter is mounted in a standard field emission microscope (FEM) with an emitter screen distance of 1 cm [5, 7-9]. The emission images have been directly photographed from a phosphor screen coated by tin oxide layers. All experiments have been performed under a very low pressure ~10^{-7} Pa, which is the ultra-high vacuum (UHV) that requires to be baked at temperatures about 453 K for 12 hours [2,10]. Before adding the liquid nitrogen to the trap, the radius of each emitter's apex is determined from an image taken in a 30 kV SEM at magnifications up to 1000 X.

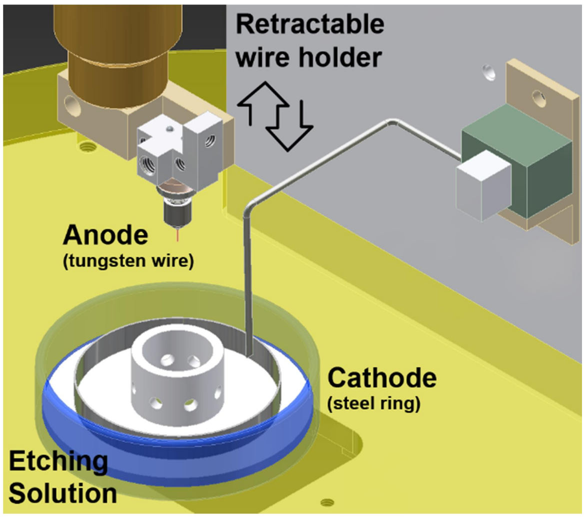

FIG. 1. The set-up of the electrolytic etching process.

Results and Discussion

The prepared tungsten micro emitters have apex radii from 100 nm to 130 nm. Presented results include VLM and SEM images of emitter's apex, I-V characteristics, as well as F-N type plots of the field emission characteristics.

Fig. 2A shows the VLM image for uncoated emitter type 1, which has an approximately hemispherical apex. The measured tip radius is 120 nm. Fig. 2B shows the VLM image for uncoated emitter type 2, which has an approximately hemispherical apex. The measured radius is 110 nm. Fig. 3 shows the emission current pattern for uncoated emitter type 1. Fig. 4 shows the emission pattern for the uncoated emitter type 2. The FEM images (emission current pattern) primarily consist of multi bright spots for the uncoated emitter type 1. The duration time among the obtained images is approx. 15 minutes, as shown in Fig. 5. The FEM images (emission current pattern) primarily consist of multi bright spots for uncoated emitter type 2. The duration time between obtaining the next images is 15 minutes, as shown in Fig. 6. I-V characteristics and FN plots for the uncoated emitters are shown in Fig. 7 A, B.

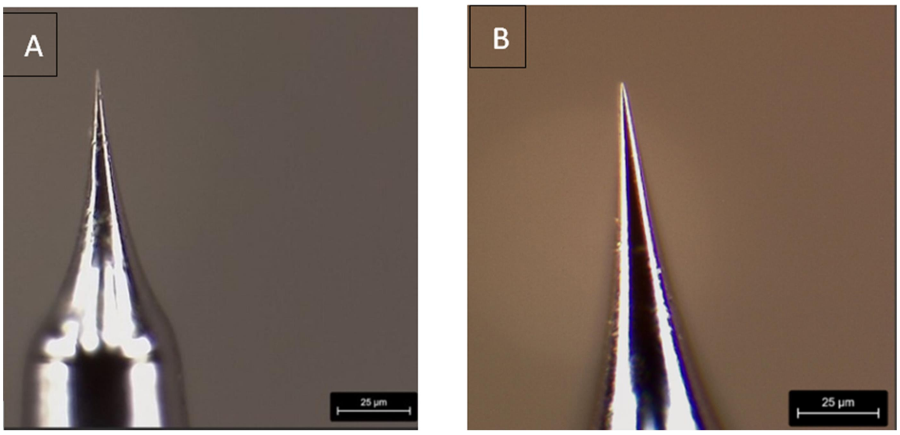

FIG. 2. A) Uncoated emitter type 1, while presenting in a visible light microscope image (X 2500). B) Uncoated emitter Type 2, while presenting in a visible light microscope image (X 2500).

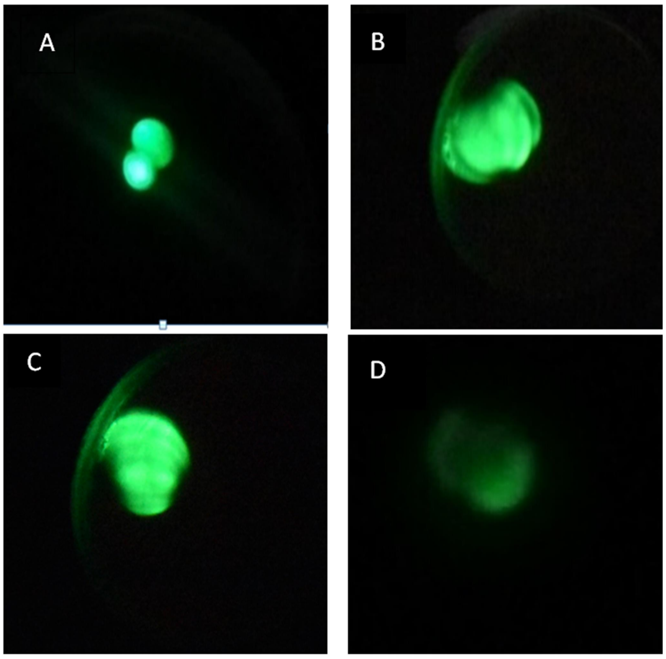

FIG. 3. Electron emission pattern for uncoated emitter type 1. A) Emission current 1.3 µA, applied voltage 1600 V. B) Emission current 0.8 µA, applied voltage 1400 V. C) Emission current 0.6 µ A, applied voltage 1200 V. D) Emission current 0.4 µA, applied voltage 1100 V.

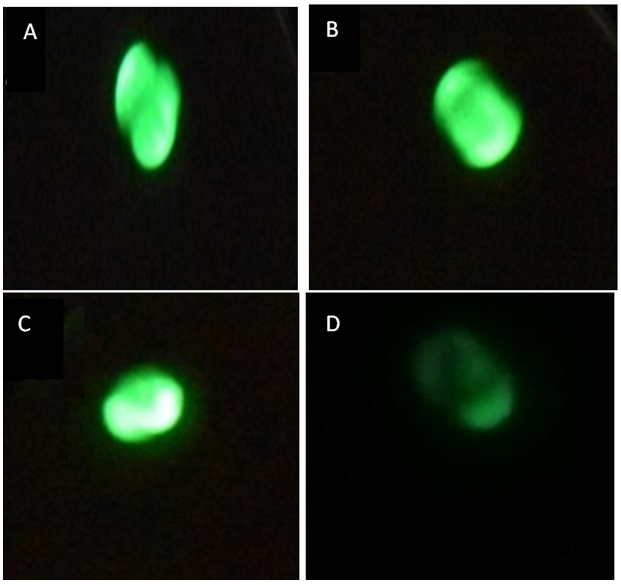

FIG. 4. Electron emission pattern for uncoated emitter type 2. A) Emission current 1.5 μA, applied voltage 1600 V. B) Emission current 1.2 μA, applied voltage 1400 V. C) Emission current 0.7 μA, applied voltage 1200 V. D) Emission current 0.3 μA, applied voltage 1100 V.

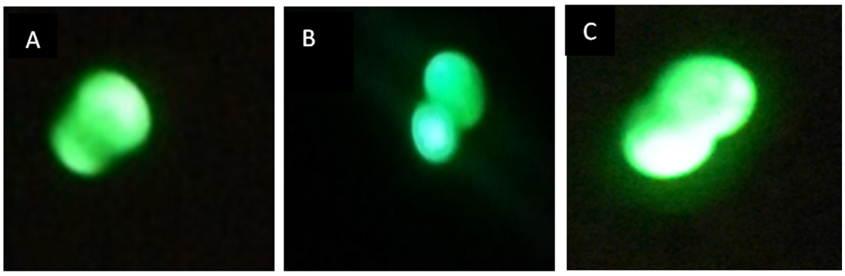

FIG. 5. The stability structure pattern for uncoated emitter type 1, at emission current 2 μA, applied voltage 1900 V. The duration time between obtaining the next images is 15 minutes.

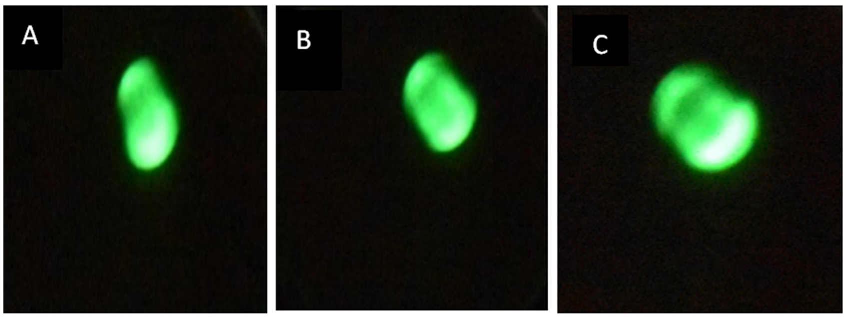

FIG. 6. The stability structure pattern for uncoated emitter type 2, at emission current 3 μA, applied voltage 1900 V. The duration time between obtaining the next images is 15 minutes.

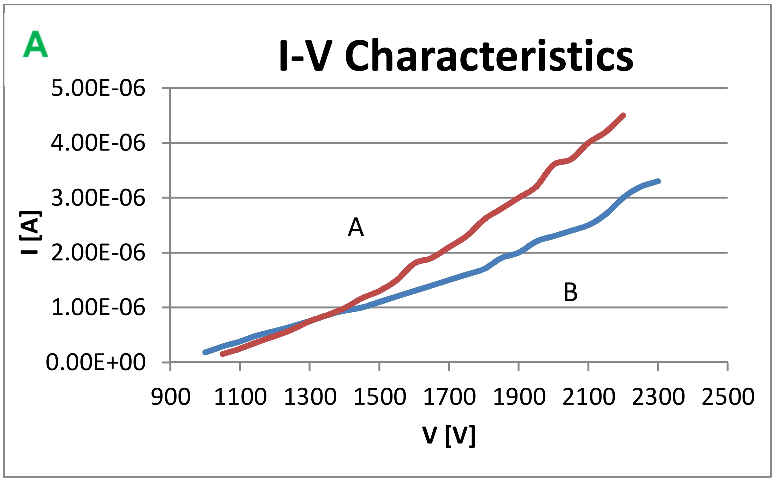

FIG. 7. A. I –V characteristics for uncoated emitters, curve A for uncoated W- emitter type 1 of tip radius 120 nm. Curve B for uncoated W- emitter type 2 of tip radius 110 nm.

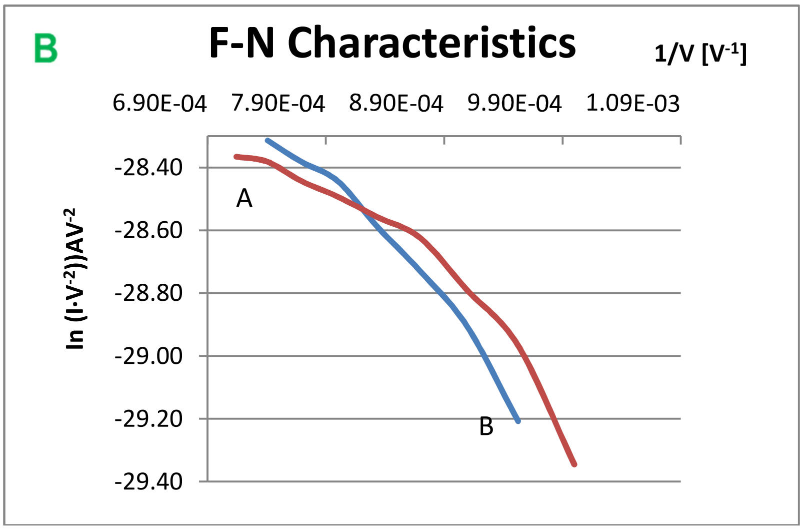

FIG. 7. B. F-N characteristics for uncoated W- emitters. Curve A for emitter type 1. Curve B for emitter type 2.

The comparison of similarity of slope for the emitters in the I-V and F-N plots (as shown in Fig. 7 A, B) shows the extent of similarity of the radius of the tips together. This has helped study the electron emission after coating the emitters with two various types of epoxy (UPR- 4 resin and Epoxylite 478 resin) under similar operational conditions, such as the thickness of the risen layer, the baking temperature and vacuum.

Fig. 8A shows the SEM image for emitter type 1 after being coated with Epoxylite UPR-4 resin, which has an approximately hemispherical apex. The tip radius was 120 nm and the Epoxylite UPR- 4 resin layer was uniformly distributed on a tip apex with a thickness of 60 nm. Fig. 8B shows the SEM image for emitter type 2 after being coated with Epoxylite 478 resin, which has an approximately hemispherical apex. The measurement radius was 110 nm and the Epoxylite 478 resin layer was uniformly distributed apex with a thickness of 60 nm. Fig. 9 shows the images for electron emission pattern for emitter type 1 after being coated with a 60-nm thick layer of Epoxylite UPR-4 resin, while Fig. 10 shows the images for electron emission pattern for emitter type 2 after being coated with a 60-nm thick layer of Epoxylite 478 resin. The images have been taken for the emission patterns at the switch-on voltage and when the voltage was regularly decreased. The FEM images primarily consist of a single bright spot for emitter type 1, as shown in Fig. 11. The FEM images primarily consist of a single bright spot for emitter type 2, as shown in Fig. 12.

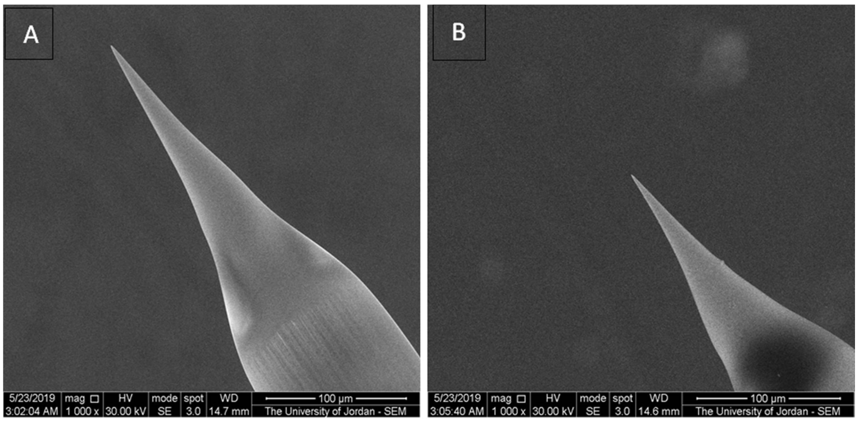

FIG. 8. A) SEM image at magnification (X 1000) for emitter type 1 after being coated with Epoxylite UPR- 4 resin. The measurement radius was 120 nm and the Epoxylite UPR- 4 resin layer was uniformly distributed tip apex with a thickness of 60 nm. B) SEM image at magnification (X 1000) for emitter type 2 after being coated with Epoxylite 478 resin. The measurement radius is 110 nm and the Epoxylite 478 resin layer was uniformly distributed tip apex with a thickness of 60 nm.

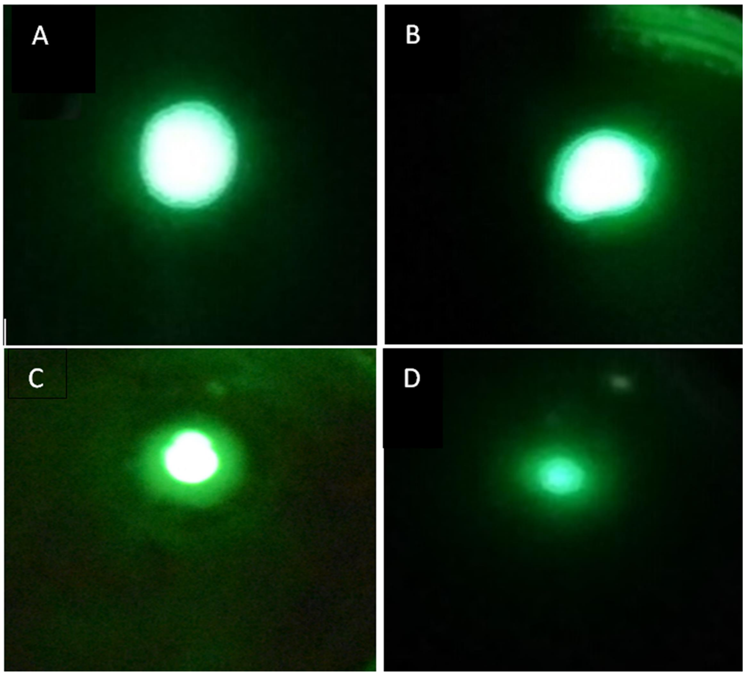

FIG. 9. Electron emission pattern for emitter type 1 after being coated with a 60-nm thick layer of Epoxylite UPR- 4 resin: A) emission current 2 µA, applied switch-on voltage 1250 V. B) emission current 1.7 µA, applied voltage 1150 V. C) emission current 1 µ, applied voltage 850 V. D) emission current 0.5 µA, applied voltage 650 V.

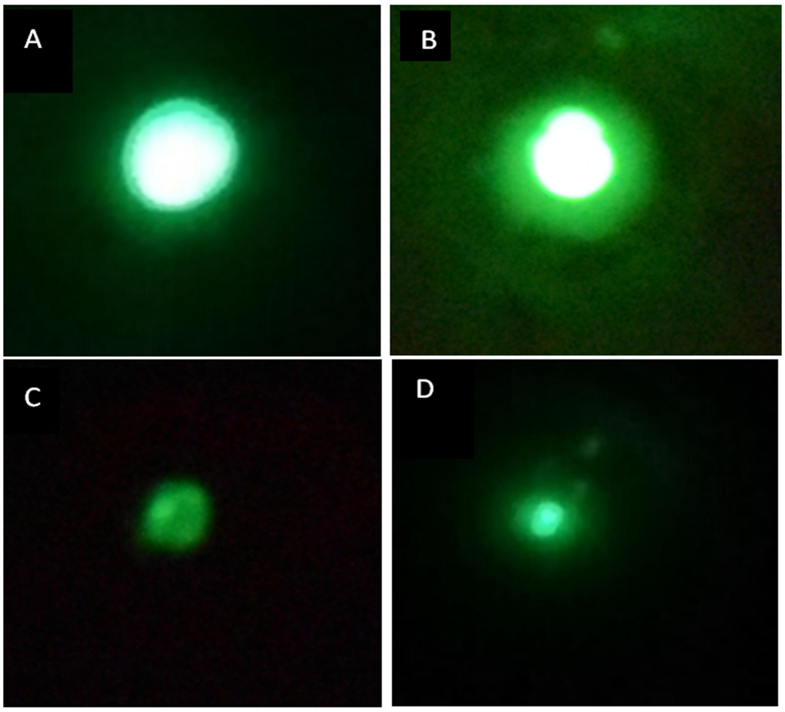

FIG. 10. Electron emission pattern for emitter type 1 after being coated with a 60-nm thick layer of Epoxylite 478 resin: A) emission current 2.3 µA, applied switch-on voltage 1150 V. B) emission current 2 µA, applied voltage 1050 V. C) emission current 1.8 µA, applied voltage 800 V. D) emission current 0.5 µA, applied voltage 650 V.

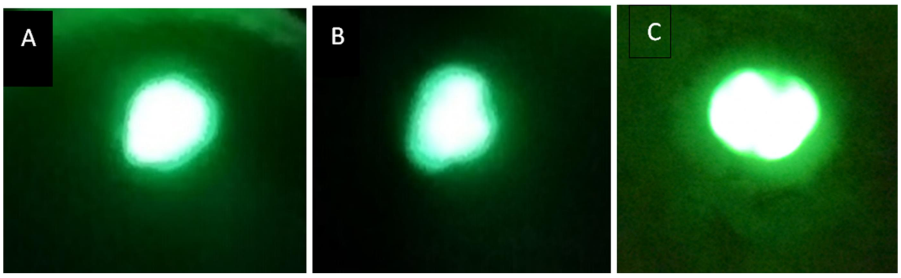

FIG. 11. The stability structure pattern for emitter type 1 after being coated with a 60-nm thick layer of Epoxylite UPR- 4 resin at emission current 1.7 µA and applied voltage 1100 V. The duration time between obtaining images is 15 minutes.

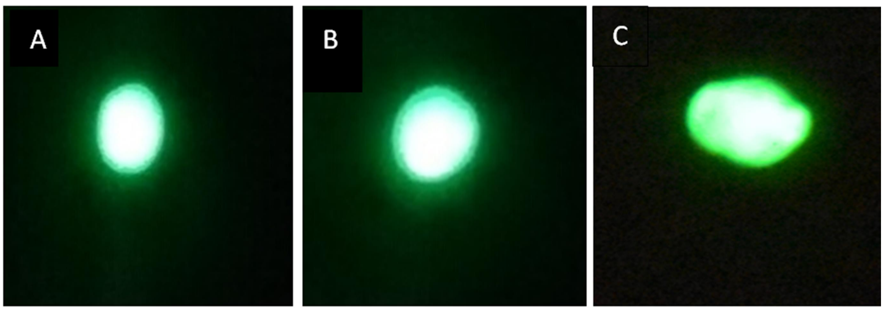

FIG. 12. The stability structure pattern for emitter type 2 after being coated with a 60-nm thick layer of Epoxylite 478 resin at emission current 2.2 µA and applied voltage 1100 V. The duration time between obtaining images is 15 minutes.

From the comparison of the emission current patterns, emission current stability structure patterns and SEM images showing the tip geometry and surface, it is concluded that emitter type 2 coated with a 60-nm thick layer of Epoxylite 478 resin has a higher emission current and is more stable compared to emitter type 1 coated with a 60-nm thick layer of Epoxylite UPR- 4 resin.

Fig. 13 shows I-V characteristics for the emitters being coated with an epoxy thin layer. For emitter type 1 coated with a 60-nm thick layer of Epoxylite UPR- 4 resin, the switch-on phenomenon occurs at V_{SW} = 1250 V and the emission current I_{SW} = 3.2μA, by decreasing the voltage of the line region of F-N plot that extends down to V_{SAT} = 800 V with an emission current I_{SAT} = 1.12 μA, by decreasing the voltage of the emission current that vanishes at V_{TH} = 550 V with an emission current I_{Th} = 46.7 PA. For emitter type 2 coated with a 60-nm thick layer of Epoxylite 478 resin, the switch-on phenomenon occurs at V_{SW} = 1150 V and the emission current I_{SW} = 3.3 μA, by decreasing the voltage of the line region of F-N plot that extends down to V_{SAT} = 600 V, with an emission current I_{SAT} = 1.08 μA, by decreasing the voltage of the emission current that vanishes at V_{TH} = 400 V, with an emission current I_{Th} = 22.3 PA. The F-N plots for the two emitters after being coated are as shown in Fig. 14.

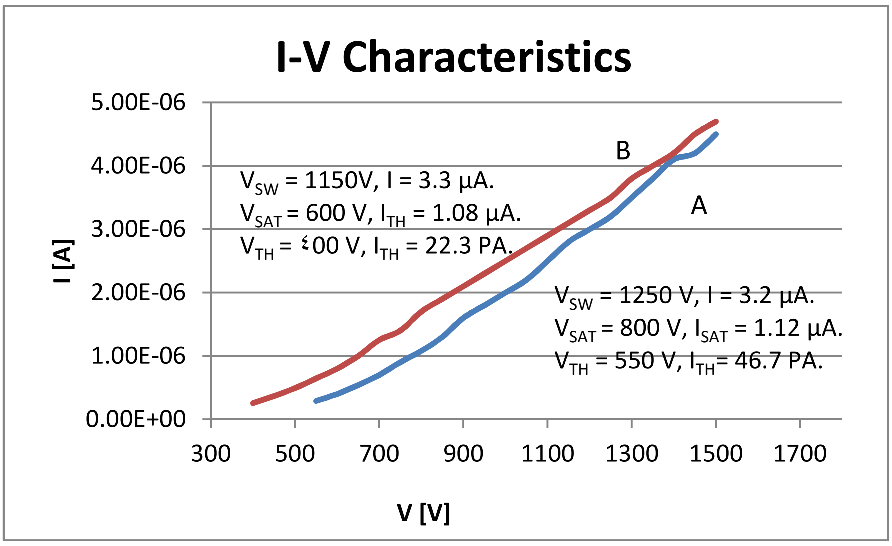

FIG. 13. Curve A is the l-V characteristics for emitter type 1 after being coated with a 60-nm thick layer of Epoxylite UPR- 4 resin. B) The l-V characteristics for emitter type 2 after being coated with a 60-nm thick layer of Epoxylite 478 resin.

From a practical point of view, the results highlighted that the switch-on voltage and threshold voltage for emitter type 2 were significantly lower than the switch-on voltage and threshold voltage for emitter type 1. Likewise, the emission current from emitter type 2 was greater than that from emitter type 1. Besides, based on the comparison of the F-N plots, it turns out that emitter type 2 leads to a decrease in the slope of these plots more than the decrease in the slope for emitter type 1 [2, 14].

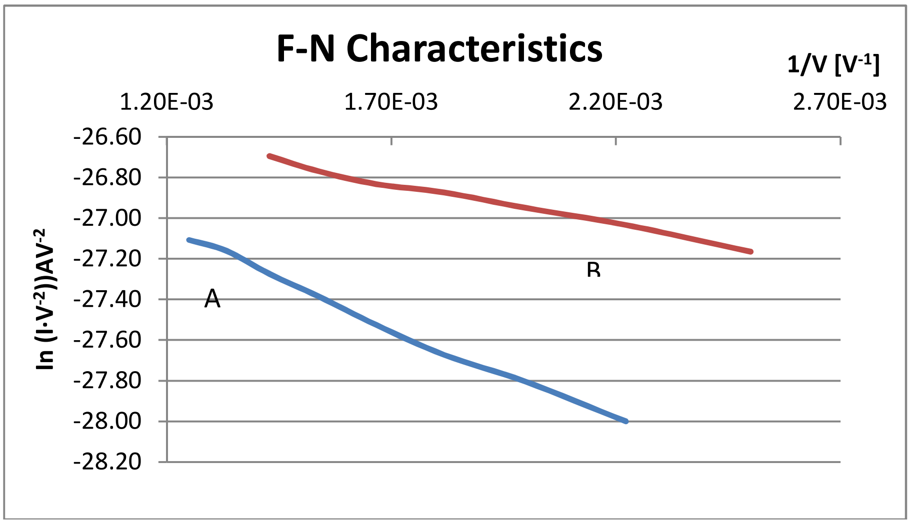

FIG. 14. Curve A shows the Fowler-Nordheim plots of emitter type 1(Epoxylite UPR- 4 resin). Curve B shows the Fowler-Nordheim plots of emitter type 2 (Epoxylite 478 resin).

Conclusion

In a nutshell, in composite emitters consisting of clean tungsten tips coated with various types of epoxy resins, the field emission characteristics of a tungsten electron source have been intrinsically changed by coating the tips with a thin layer of epoxy resins. This is in line with the results obtained from similar studies [2, 5, 15]. This change in characteristics varies depending on the type of epoxy resins used in coating the tungsten tips. More importantly, this is evident by comparing the effects of epoxy resins used in this work (Epoxylite 478 resin and UPR-4 resin).

Acknowledgments

The authors would like to thank the Deanship of Academic Research at Mu'tah University for supporting this work through research project number 241/19/120.

The research infrastructure was funded by the Czech Academy of Sciences (project RVO: 68081731).

References

[1] Forbes, R.G., Deane, J.H., Hamid, N. and Sim, H.S., Journal of Vacuum Science & Technology, 22 (2004) 1222.

[2] Mousa, M.S., Latham, R.V., Le Journal de Physique Colloques, 47 (1986) 139.

[3] Alnawasreh, S., Mousa, M.S. and Al-Rabadi, A.N., Jordan J. Phys., 8 (2) (2015) 95.

[4] Knápek, A., Sýkora, J., Chlumská, J. and Sobola, D., Microelectronic Engineering, 173 (2017) 42.

[5] Sergeev, E., Knapek, A., Grmela, L. and Šikula, J., International Conference on Noise and Fluctuations (ICNF), (2013) 1- 4.

[6] Al-Qudah, A.M., Mousa, M.S. and Fishcher, A., IOP Conf. Series: Materials Science and Engineering, 92 (2015) 12.

[7] Al-Qudah, A.M. and Mousa, M.S., Applied Microscopy, 3 (2016) 30.

[8] Latham, R.V. and Salim, M.A., Journal of Physics E: Scientific Instruments, 2 (1987) 181.

[9] Meza, J.M., Lubin, C., Thoyer, F., Rosales, K.V., Espinoza, A.G., Martin, F. and Cousty J., Carbon, 8 (2015) 363.

[10] Madanat, M.A., Mousa, M.S., Al-Rabadi, A.N. and Fischer, A., Jordan J. Phys., 8 (2) (2015) 79.

[11] Zhou, W., Wang, Z.L., Eds., "Scanning Microscopy for Nanotechnology", (Springer, 2007).

[12] FEI Company, "An Introduction to Electron Microscopy", (2010).

[13] Mousa, M.S., Surface and Interface Analysis, 39 (2007) 102.

[14] Mayer, A., Mousa, M.S. and Vigneron, J.P., Ultramicroscopy, 89 (2001) 95.

[15] Al-Qudah, A.M., Alnawasreh, S.S., Madanat, M.A., Trzaska, O., Matykiewicz, D., Alrawshdeh, S.S., Hagmann, M.J. and Mousa, M.S., Jordan J. Phys., 11 (1) (2018) 59.